Cellular/Molecular

The *Drosophila* Metabotropic Glutamate Receptor DmGluRA Regulates Activity-Dependent Synaptic Facilitation and Fine Synaptic Morphology

Laurent Bogdanik,[1]* Ralf Mohrmann,[2]* Ariane Ramaekers,[1] Joël Bockaert,[1] Yves Grau,[1] Kendal Broadie,[2] and Marie-Laure Parmentier[1]

[1]Laboratoire de Génomique Fonctionnelle, Centre National de la Recherche Scientifique, Unité Propre de Recherche 2580, 34094 Montpellier Cedex 05, France, and [2]Department of Biological Sciences, Kennedy Center for Research on Human Development, Vanderbilt Brain Institute, Vanderbilt University, Nashville, Tennessee 37232

In vertebrates, several groups of metabotropic glutamate receptors (mGluRs) are known to modulate synaptic properties. In contrast, the *Drosophila* genome encodes a single functional mGluR (DmGluRA), an ortholog of vertebrate group II mGluRs, greatly expediting the functional characterization of mGluR-mediated signaling in the nervous system. We show here that DmGluRA is expressed at the glutamatergic neuromuscular junction (NMJ), localized in periactive zones of presynaptic boutons but excluded from active sites. Null *DmGluRA* mutants are completely viable, and all of the basal NMJ synaptic transmission properties are normal. In contrast, *DmGluRA* mutants display approximately a threefold increase in synaptic facilitation during short stimulus trains. Prolonged stimulus trains result in very strongly increased (~10-fold) augmentation, including the appearance of asynchronous, bursting excitatory currents never observed in wild type. Both defects are rescued by expression of DmGluRA only in the neurons, indicating a specific presynaptic requirement. These phenotypes are reminiscent of hyperexcitable mutants, suggesting a role of DmGluRA signaling in the regulation of presynaptic excitability properties. The mutant phenotypes could not be replicated by acute application of mGluR antagonists, suggesting that DmGluRA regulates the development of presynaptic properties rather than directly controlling short-term modulation. *DmGluRA* mutants also display mild defects in NMJ architecture: a decreased number of synaptic boutons accompanied by an increase in mean bouton size. These morphological changes bidirectionally correlate with DmGluRA levels in the presynaptic terminal. These data reveal the following two roles for DmGluRA in presynaptic mechanisms: (1) modulation of presynaptic excitability properties important for the control of activity-dependent neurotransmitter release and (2) modulation of synaptic architecture.

Key words: **G-protein-coupled receptor; neuromuscular junction; presynaptic; bouton; excitability; synaptic modulation; facilitation; augmentation**

Introduction

In the mammalian brain, glutamatergic synapses mediate the majority of excitatory transmission, and changes in their transmission efficacy and architecture are thought to underlie higher cognitive processes (Yuste and Bonhoeffer, 2001; Lynch, 2004). Fast glutamatergic transmission is mediated by ionotropic glutamate receptors (iGluRs), but synaptically released glutamate also activates metabotropic glutamate receptors (mGluRs), which signal via slower G-protein-coupled pathways. In mammals, eight mGluRs fall into three groups based on sequence homology, pharmacological properties, and downstream signaling pathway (Conn and Pin, 1997). Group I mGluRs activate G_q-proteins, whereas group II/III mGluRs activate G_i/G_o-proteins. The different mGluR classes are involved in multiple physiological processes, including regulation of neuronal excitability, excitotoxicity, and synaptic plasticity. Group I receptors are localized in the postsynapse (Baude et al., 1993), in which they participate in modulation of NMDA receptor function (Anwyl, 1999). Group II receptors (i.e., mGluR2 and mGluR3) often appear in presynaptic membranes, away from synaptic sites (Lujan et al., 1997; Shigemoto et al., 1997), in which they induce presynaptic inhibition during intense stimulation (Conn and Pin, 1997; Scanziani et al., 1997). The physiological role of mGluR subtypes has been addressed in knock-out mice, revealing region-specific functions, including modulation of long-term potentiation and depression (Ozawa et al., 1998). However, the function of mGluRs in the

Received April 2, 2004; revised Aug. 2, 2004; accepted Aug. 3, 2004.

This work was supported by a fellowship from the Ministère de la Recherche (L.B.), by grants from Centre National de la Recherche Scientifique to the Laboratoire de Génomique Fonctionnelle, and by National Institutes of Health Grant GM54544 (K.B.). We thank W. Gehring, L. Wallrath, V. Budnik, C. O'Kane, C. Schuster, C. F. Wu, and J. Knöblich for fly stocks and Y. Kidokoro and C. Eroglu for antibodies. We thank members of the Broadie Laboratory for advice and input on this manuscript, T. Parks (University of Utah) for advice on argiotoxin, and NPS Pharmaceuticals for supplying the toxin. We also thank members of the J. Bockaert and J.-M. Dura laboratories for their input during this work. We give special thanks to the editor and reviewer for helpful comments and suggestions.

*L.B. and R.M. contributed equally to this work.

Correspondence should be addressed to Marie-Laure Parmentier, Laboratoire de Génomique Fonctionnelle, Centre National de la Recherche Scientifique, Unité Propre de Recherche 2580, 141 Rue de la Cardonille, 34094 Montpellier Cedex 05, France. E-mail: mlparmentier@ccipe.cnrs.fr.

A. Ramaekers' present address: Département de Biologie, Université de Fribourg, Pérolles, Chemin du Musée 10, CH-1700 Fribourg, Switzerland. E-mail: ariane.ramaekers@unifr.ch.

DOI:10.1523/JNEUROSCI.2724-04.2004

 0270-6474/04/249105-12$15.00/0

structural synaptic plasticity remains essentially unknown (Vanderklish and Edelman, 2002).

The *Drosophila* neuromuscular junction (NMJ) has been instrumental in revealing mechanisms of glutamatergic synapse development, transmission, and activity-dependent plasticity (Packard et al., 2003; Rohrbough et al., 2003). The iGluRs at this synapse are well characterized (Schuster et al., 1991; Petersen et al., 1997; DiAntonio et al., 1999; Sigrist et al., 2002; Marrus et al., 2004), but there has been no genetic analysis of *Drosophila* mGluRs. The *Drosophila* genome possesses two predicted mGluR genes. *Drosophila metabotropic glutamate receptor A* (*DmGluRA*) is an mGluRs2/3 ortholog (Parmentier et al., 1996). DmGluRA shares the pharmacological profile of group II mGluRs and couples to G_i/G_o (Parmentier et al., 1996). The recently characterized product of the other locus, DmXR, is not detectably activated by L-glutamate (Mitri et al., 2004). Thus, DmGluRA is the only functional mGluR encoded by the sequenced *Drosophila* genome. This provides the unique opportunity to study the entire mGluR-dependent processes in *Drosophila* through mutation of a single gene.

In this study, we characterize for the first time *Drosophila DmGluRA* mutants. We were especially interested in the question of whether DmGluRA has a function at the well characterized NMJ, as a mechanism to sense glutamate release and feedback to regulate synaptic architecture, excitability, and/or transmission properties. We show here that DmGluRA is expressed presynaptically, in local punctate clusters, in accordance with a previous pharmacological study (Zhang et al., 1999). In null *DmGluRA* mutants, the NMJ displays entirely normal basal transmission properties but displays pronounced defects in activity-dependent neurotransmitter release. In particular, synaptic facilitation is increased during short trains of high-frequency stimulation, and, if the trains are prolonged, mutant synapses display remarkably increased asynchronous excitatory currents. In addition, we show that presynaptic DmGluRA governs the fine-tuning of the NMJ morphological structure. These results demonstrate that the ability to sense glutamate release, via a presynaptic DmGluRA-dependent feedback mechanism, is important for sculpting synaptic architecture and regulating presynaptic excitability properties required for appropriate activity-dependent glutamate release.

Materials and Methods

Fly strains and genetics. Generation of the *DmGluRA* mutant was as follows: using PCR rescue analysis and sequencing, a P(white+) element insertion (Cryderman et al., 1998) on the fourth chromosome was identified in the homozygous viable line P39C42 (obtained from L. Wallrath, University of Iowa, Iowa City, IA). This transposon was inserted 5.94 kb upstream of the translation initiation codon of the *DmGluRA* gene. The P-element was mobilized using P[ry+, Δ2–3](99B) as a transposase source (Robertson et al., 1988) according to standard procedures. One hundred thirty-five independent white revertant lines were analyzed by PCR using genomic primers as follows: forward, 5′-GATCAGGGCCAAGGTGTGTCCAGC-3′ and 5′-AAGCCGCTTTGGCGTTGC-3′; reverse, 5′-GCTCACTCCCACACAAGCGC-3′ and 5′-GAGCCCAATGATCCGTGGAAAGCG-3′. One imprecise excision deletion event affecting the *DmGluRA* transcription unit was recovered, called $DmGluRA^{112b}$ (abbreviated 112b). This homozygous viable mutant stock was maintained as *yw;* $DmGluRA^{112b}$. A precise P-element excision line, called $DmGluRA^{2b}$ (abbreviated 2b), was maintained as *yw;* $DmGluRA^{2b}$ and served as control of the same genetic background. The integrity of the *DmGluRA* genomic region in the 2b line was verified by sequencing PCR amplification from genomic DNA. Reverse transcription-PCR experiments showed that *DmGluRA* transcription levels in 2b flies were indistinguishable from wild-type lines (data not shown). A genomic deletion covering the *DmGluRA* region *Df(4)O2* was obtained from W. Gehring (Biozentrum, Basel, Switzerland); the deficiency is not detectable by chromosome cytology. Southern blot analysis revealed that *Df(4)O2* deletes the entire *DmGluRA* coding region. The *Df(4)O2* deletion line was maintained as *yw;* $Df(4)O2/Ci^{D}$ *spa*. $DmGluRA^{112b}/Df(4)O2$ *spa* and $DmGluRA^{2b}/Df(4)O2$ *spa* larvae were obtained as follows. A *UAS mCD8::GFP;* $Df(4)O2/Ci^{D}$ *spa* stock was crossed to a *UAS mCD8::GFP; OK107 GAL4* stock (Lee et al., 1999). Non-Ci^{D} males (*mCD8::GFP; Df(4)O2 spa/OK107 GAL4*) were selected and mated with either the 112b mutant or 2b control line, and nonfluorescent larvae were selected for analysis.

Transgenic RNA interference (RNAi) lines were generated by constructing an original AB–AB–BA repeat of an 800 bp fragment from the KosDmGRA vector (Parmentier et al., 1996) instead of the usual AB–BA hairpin. Such a construction was easier to obtain during the successive subcloning steps, and the bacterial clones of the final construct were also more stable. The 800 bp fragment was amplified with modified primers carrying restriction sites. 5′-*Eco*RI–*Kpn*I DA1 primer sequence is as follows: forward, 5′-GGCCGAATTCGGTACCAGACAAGCATCAACCAACGAC-3′; and the 3′-*Bgl*II DA2 primer sequence is as follows: reverse, 5′-GAAGATCTTCACCATAAGATCCTTCCGAA-3′. This AB amplicon (see Fig. 2) ranges from nucleotide 90 to nucleotide 882 of the cDNA. P-element-mediated DNA transformations were performed using standard methods. Several independent UAS-DmGluRA-RNAi transgenic lines were established. DmGluRA-RNAi^{325} and DmGluRA-RNAi^{1061} transgenes are respectively located on the first and third chromosomes. The double-homozygous DmGluRA-RNAi^{325}; DmGluRA-RNAi^{1061} strain was constructed and used in most of the experiments. Two independent UAS-DmGluRA transgenic strains (Ramaekers et al., 2001), each carrying one insertion on the second or on the third chromosome, were used. The UAS-DmGluRA and UAS-DmGluRA-RNAi constructs were driven by either the two neuronal (presynaptic at NMJ) GAL4 lines BG380-GAL4 (Budnik et al., 1996) and OK6-GAL4 (Aberle et al., 2002) or the muscle (postsynaptic at NMJ) driver MHC82-GAL4 (Schuster et al., 1996a).

The double-mutant strain eag^{1} Sh^{120} was a kind gift from C. F. Wu (University of Iowa, Iowa City, IA). The recessive loss-of-function Gβ13F mutant allele ($G\beta13F^{\Delta 1-96A}$), which is rescued by a transgene containing the Gβ13F transcription unit and 1.1 kb of upstream sequence (Schaefer et al., 2001), was a kind gift from J. Knoblich (Research Institute of Molecular Pathology, Vienna, Austria).

Animal rearing. To control for rearing variation, parental females of each genotype were allowed to lay eggs on an agar plate for 24 hr at 25°C, and 50 first instar larvae were collected just after hatching and placed into vials with standard medium at 25°C to develop until the third instar. Wandering third instar larvae were then collected for all of the analyses.

Quantification of NMJ structure. Dissected third instar preparations were stained with rabbit anti-HRP and Cy3-conjugated anti-rabbit. Synaptic boutons on muscles 6/7 and 12/13 of the A2 segment were counted on a wide-field fluorescence microscope (Axiophot; Zeiss, Oberkochen, Germany) at 100× magnification. A picture of the inner surface of muscle 6/7 was taken at 20× magnification to quantify the muscle area. The normalized bouton number was calculated by dividing bouton numbers by muscle surface area (Schuster et al., 1996b). Data were expressed in percentage of the control of each experiment to compensate for variations between different experiments. For bouton size quantification, NMJs were imaged with a confocal microscope (model 1024; Bio-Rad, Hercules, CA; Centre Régional d'Imagerie Cellulaire, Montpellier, France) at 40× magnification. Each bouton was then delineated by hand, and its area was calculated by the NIH ImageJ software. All the quantifications of synapse morphology were performed blind of genotype.

Immunocytochemistry. The following antibodies were used: rabbit anti-HRP (1:2000; Sigma, St. Louis, MO), mouse monoclonal anti-DmGluRA antibody 7G11 (1:400; a gift from C. Eroglu, European Molecular Biology Laboratory, Heidelberg, Germany), rabbit anti-DGluR-IIA DM2 (1:2000; a kind gift from Y. Kidokoro, Gunma University, Gunma, Japan), FITC, or Cy3-conjugated anti-rabbit or anti-mouse (Vector Laboratories, Burlingame, CA). 7G11 immunoreactivity was visualized using a Tyramide Amplification kit (PerkinElmer Life Sciences,

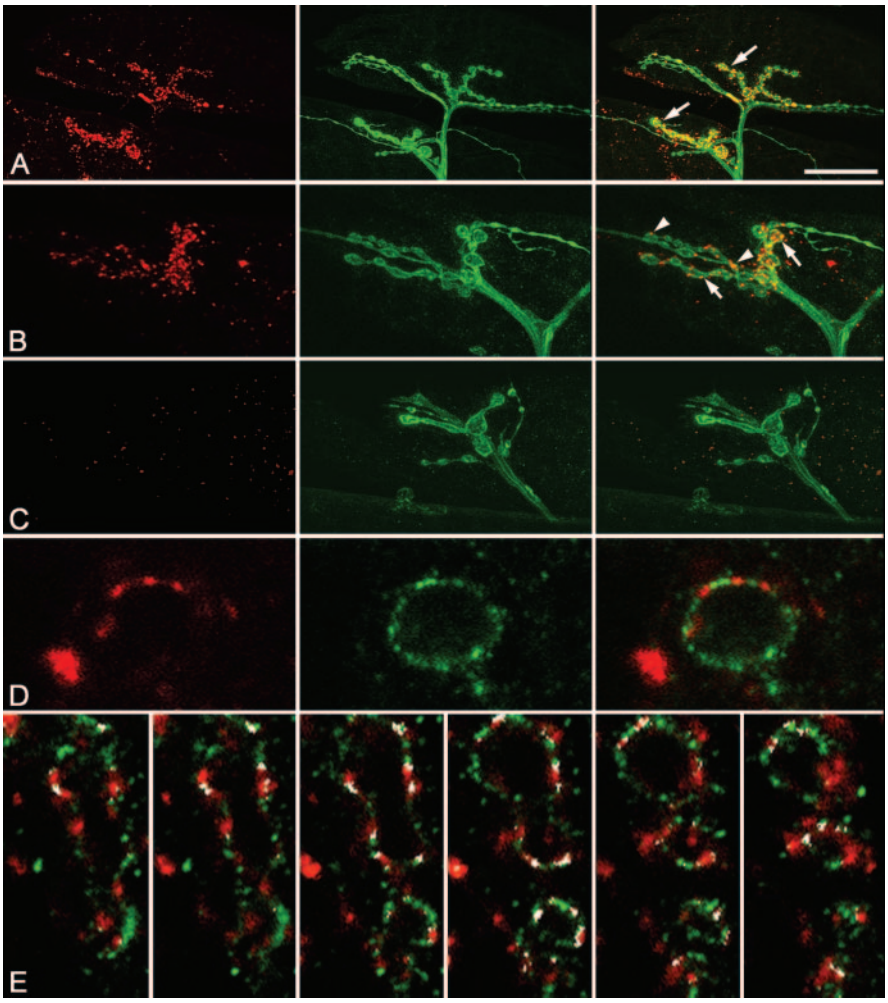

Figure 1. Expression of DmGluRA at the NMJ. *A*, DmGluRA (red) and HRP (green) immunoreactivity at the NMJ of wild-type muscles 12 and 13. Merge of both images (right). DmGluRA-positive patches are clearly visible at type I boutons (arrows). *B*, Higher magnification of a terminal branch with DmGluRA (red) and HRP (green) stainings. DmGluRA-positive patches are visible at type Ib (arrows) and type Is (arrowheads) boutons. Merged images (right) show a strong colocalization of DmGluRA immunoreactivity and the presynaptic marker HRP (yellow). *C*, DmGluRA (red) and HRP (green) immunoreactivity at the NMJ of *DmGluRA*^{112b} mutants. Synaptically localized DmGluRA-positive patches are absent. Spot-like immunoreactivity on the muscle surface most likely represents unspecific antibody binding. Merged images (right). Note that *DmGluRA*^{112b} NMJ display less and bigger boutons than control NMJ shown in *B*. *D*, Double staining of DmGluRA (red) and the glutamate channel receptors DGluR-IIA (green) shows a complementary distribution of clusters of each receptor at the level of a single synaptic bouton. *E*, Double staining of DmGluRA (red) and the glutamate channel receptors DGluR-IIA (green), with the colocalization areas colored in white (obtained with NIH ImageJ software). From left to right, Successive confocal planes every 0.5 μm of the same axonal branch. Note that colocalization only occurs at the periphery of DmGluRA and DGluR-IIA clusters. Scale bar (in *A*): *A*, 30 μm; *B*, *C*, 15 μm; *D*, 2.5 μm; *E*, 5 μm.

Emeryville, CA), using biotinylated anti-mouse antibody (1:100; Vector Laboratories) and streptavidin–HRP (1:100). HRP enzymatic activity was detected with Cy3–tyramide as substrate (1:50; 3 min incubation). 7G11-immunoreactive NMJs were quantified by counting the number of labeled NMJs on muscle 4 from segments A2 to A6 in at least six larvae.

Western blotting. For membrane protein extraction, 40 adult *Drosophila* heads were homogenized in lysis buffer (in mM): 20 Tris HCl, pH 7.4, 250 sucrose, 2 $MgCl_2$, and 500 NaCl. Homogenates were centrifuged at 200 $\times$ *g* for 5 min. Supernatant was sonicated and centrifuged at 13,000 $\times$ *g* for 30 min. The pellet was resuspended in 100 μl of radioimmunoprecipitation assay buffer (in mM: 50 Tris HCl, pH 7.4, 150 NaCl, 2.5 EDTA, 1% Triton X-100, and 0.1% SDS) and placed under gentle agitation at 4°C for 30 min. After a last centrifugation at 13,000 $\times$ *g* for 30 min, supernatant was collected. One microliter of the supernatant was used for protein dosage by bicinchoninic acid assay (Sigma). Equal amounts of membrane proteins (100 μg) of each strain extract were added with 6$\times$ Laemmli buffer and loaded on a 7.5% SDS–polyacrylamide gel. 7G11 anti-DmGluRA antibody (1:1000) and HRP-conjugated anti-rabbit (1:3000; Amersham Biosciences, Arlington Heights, IL) were used for immunoblotting. The ECL detection kit (Amersham Biosciences) was used.

Electrophysiology. Standard NMJ recordings in third instar larvae were performed as described previously (Rohrbough et al., 1999). Briefly, third instar larvae were dissected in calcium-free standard saline (in mM: 128 NaCl, 2 KCl, 4 $MgCl_2$, 70 sucrose, 5 HEPES, pH 7.1) and directly transferred to standard saline containing either 1.8 or 0.15 mM Ca^{2+} for recording, as indicated. The temperature during all of the recordings was 18°C. All of the recordings were done in the anterior abdominal segment 3 in muscle 6 using two-electrode voltage-clamp (TEVC) techniques (Axoclamp 2B amplifier; Axon Instruments, Foster City, CA). The holding potential was set at -60 mV in all of the experiments. Intracellular recording electrodes were filled with 3 M KCl and typically had a resistance of $\sim$10 MΩ. Excitatory junction currents (EJCs) were evoked by application of brief stimuli (0.4–0.5 msec), or trains of stimuli, from a Grass Instruments (Quincy, MA) S88 stimulator to the cut motor nerve using a glass suction electrode. For drug application, preparations were incubated for 20 min in a bath solution containing the pharmacological agent, as indicated. Before recording, the bath solution was exchanged for fresh saline containing the drug. To obtain argiotoxin-blocking rates, synapses were stimulated for 1 min at 5 Hz before the amplitude reduction was quantified. Action potentials were recorded extracellularly from nerves using a differential amplifier (AC/DC amplifier model 3000; A-M Systems, Carlsborg, WA). Data acquisition and analysis was performed using pClamp software (version 8.0; Axon Instruments). Data is presented as mean $\pm$ SEM.

Results

DmGluRA is expressed at the glutamatergic NMJ

In previous work (Ramaekers et al., 2001), we were unable to detect the expression of DmGluRA at the *Drosophila* larval NMJ. However, recent pharmacological studies strongly inferred the presence of functional metabotropic glutamate receptors at this synapse (Zhang et al., 1999; Hou et al., 2003). Because DmGluRA is the only functional metabotropic glutamate receptor encoded within the sequenced *Drosophila* genome (Mitri et al., 2004), it seemed probable that previous experimental limitations prevented detection of the receptor at the NMJ. Panneels et al. (2003) recently described a superior new monoclonal antibody (7G11) directed against the extracellular domain of DmGluRA. We used this new probe to reevaluate DmGluRA localization at NMJs of mature third instar larvae.

Thanks to a tyramide amplification system, clear DmGluRA immunoreactivity is observed at the NMJ with the 7G11 monoclonal antibody (Fig. 1). DmGluRA is detected in large immunoreactive areas, as well as smaller punctate domains at synaptic boutons, colocalizing with anti-HRP staining of the presynaptic

membrane (Fig. 1*A*,*B*). Body-wall muscles are innervated by different glutamatergic motor neurons, whose endings fall into three morphologically distinct classes: types I, II, and III (Rheuben et al., 1999). Type I glutamatergic terminals are labeled by 7G11 antibody on ventral longitudinal muscle 6/7, as well as on the other well characterized muscles 4, 12, and 13 (Fig. 1*A*). When DmGluRA expression was quantified for the muscle 4 NMJs, immunoreactivity was detected in 80 ± 7% of NMJs ($n = 7$). DmGluRA immunoreactivity is also present at the NMJs of all of the other body-wall muscles inspected (data not shown). Interestingly, our experiments show qualitative differences in the staining intensity of different bouton types: DmGluRA-immunoreactive patches were much less pronounced on type Is than on type Ib (Fig. 1*B*).

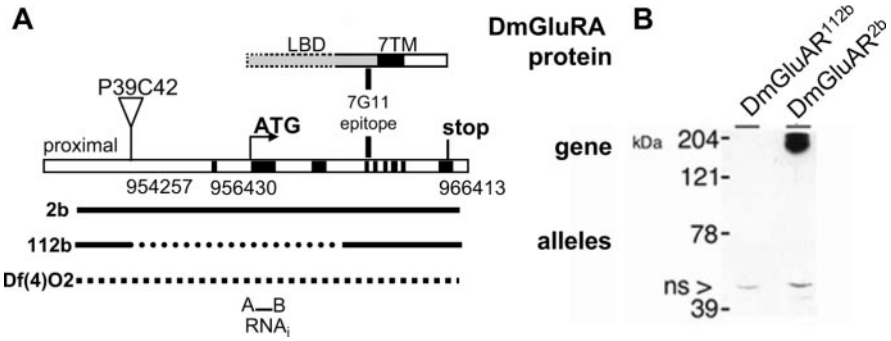

Figure 2. DmGluRA: gene structure and mutant generation. *A*, Predicted intron–exon splicing pattern of *DmGluRA* gene compiled from the comparison of genomic and cDNA sequences. The P-element P39C42 is localized 5.94 kb upstream of the translation initiation codon of *DmGluRA* (positions according to *Drosophila* genome sequence release 3.0). Line 2b contains a precise excision of P39C42. *DmGluRA*^{112b} represents an imprecise excision of the same P-element deleting the putative transcription start, the start codon, as well as part of the sequence coding for the extracellular LBD. Df(4)O2 removes the whole *DmGluRA*. The epitope recognized by 7G11 antibody is part of the extracellular domain, between the LBD and the seven transmembrane domain (7TM) (Panneels et al., 2003), and is not deleted in *DmGluRA*^{112b} allele. The sequence selected for DmGluRA-RNAi constructs is indicated at the bottom. *B*, Western blot analysis of wild-type and *DmGluRA*^{112b} head extracts with 7G11 antibody: a strong ~200 kDa band corresponding to the DmGluRA dimer is present in wild-type extracts, whereas it is absent in *DmGluRA*^{112b} mutant extracts. A 45 kDa unspecific band is present in both lanes (arrowhead), indicating a similar protein load in both lanes.

DmGluRA immunoreactivity colocalized with anti-HRP labeling of the presynaptic membrane in type I presynaptic boutons. In addition, however, DmGluRA expression often appeared to exceed the limits of the presynaptic terminals (as imaged by anti-HRP staining) (Fig. 1*A*). This can be attributable to either the amplification system used for 7G11 stainings or a partial postsynaptic localization of the receptor. We therefore tried to distinguish presynaptic and postsynaptic expression by cell-specific suppression of the receptor using GAL4-targeted *DmGluRA*-RNAi. Most interestingly, we found that RNAi driven by GAL4 drivers that are reported to express in motor neurons abolished DmGluRA immunoreactivity in 40 ± 8% ($n = 6$; $p < 0.05$) of muscle 4 NMJs compared with the control, i.e., larvae carrying the RNAi construct without any GAL4 driver ($n = 6$). In contrast, DmGluRA immunoreactivity persisted at the same level as that in control conditions when expression of RNAi was driven by the muscle-specific driver MHC-GAL4 (relative number of NMJ labeled is 117 ± 14%; $n = 7$; NS). These results suggest that DmGluRA is predominantly expressed in the presynaptic bouton membrane but cannot exclude some contribution from postsynaptic localization.

At high magnification, DmGluRA expression appears locally patchy, suggesting that the metabotropic receptors are localized in discrete clusters at synaptic boutons (Fig. 1*B*). Previous studies have shown that boutons are compartmentalized into active zones, in which exocytosis of neurotransmitter occurs, and periactive zones, regions involved in endocytosis (Koenig and Ikeda, 1996; Gonzalez-Gaitan and Jackle, 1997) as well as other functions, including growth control of the synapse (Sone et al., 2000). To determine in which compartment DmGluRA receptors are localized, NMJs were colabeled with postsynaptic markers of release sites, such as the ionotropic glutamate receptor subunit DGluR-IIA (Petersen et al., 1997; Saitoe et al., 2001). We observed that DmGluRA clusters did not colocalize with DGluR-IIA clusters (Fig. 1*D*). A quantification of the colocalization of these two classes of glutamate receptor showed that only 9.75 ± 1.75% ($n = 11$) of iGluR signal overlapped with DmGluRA signal, and 9.7 ± 2.4% (same larvae; $n = 11$) of DmGluRA signal overlapped with iGluR signal. In all of the cases, the overlap of the iGluR and DmGluRA patches (Fig. 1*E*, white pixels) occurred at the periphery of the respective clusters, indicating that iGluRs and mGluRs inhabit distinctive, essentially nonoverlapping domains (Fig. 1*E*). These results suggest that DmGluRA clusters are predominantly within the periactive zone surrounding presynaptic glutamate release sites and do not form part of the active zone domain.

In summary, these data show that DmGluRA is present at the *Drosophila* NMJ, although the receptor appears expressed at a low level compared, for example, with the abundant iGluR. Furthermore, DmGluRA expression is primarily restricted to the presynaptic compartment. DmGluRA clusters do not significantly invade the active zone domain; therefore, they do not colocalize with the D-GluRIIA receptors but rather reside in the surrounding periactive zone of the presynaptic membrane. In addition to the demonstration of staining specificity with cell-specific RNAi, the specificity of the immunostaining was also confirmed in mutant animals (Fig. 1*C*) (see below).

Generation of *DmGluRA* mutants

To assay synaptic roles of the DmGluRA receptor, we generated null mutants. The *DmGluRA* gene is localized within cytological region 102C-D on the fourth chromosome (Parmentier et al., 1996). A P(white$^+$) element, P39C42 (Cryderman et al., 1998), was found to be inserted ~6 kb upstream of the *DmGluRA* start codon (at position 954257; see Materials and Methods) (Fig. 2*A*). Using standard genetic techniques, we mobilized this transposable element and recovered an imprecise excision line called *DmGluRA*^{112b}. With PCR amplification and sequence analysis of the *DmGluRA* genomic region, we showed that the deletion removes the start codon and part of the sequence encoding the extracellular ligand-binding domain (LBD) of DmGluRA (Fig. 2*A*). This molecular characterization showed that the deletion was specific to the *DmGluRA* gene and predicted that the *DmGluRA*^{112b} mutant could not encode a functional glutamate receptor. A precise excision line, *DmGluRA*^{2b}, was identified as a control for the phenotypic analysis.

To further characterize *DmGluRA*^{112b}, the expression levels of DmGluRA protein were compared with *DmGluR*^{2b} controls by Western blot analysis. Using the 7G11 antibody, which recognizes an epitope not deleted in *DmGluRA*^{112b} mutants, no residual full-length or truncated gene product was detected in adult heads of *DmGluRA*^{112b} mutants (Fig. 2*B*). In contrast, strong expression of a dimerized form of the receptor (204 kDa) was

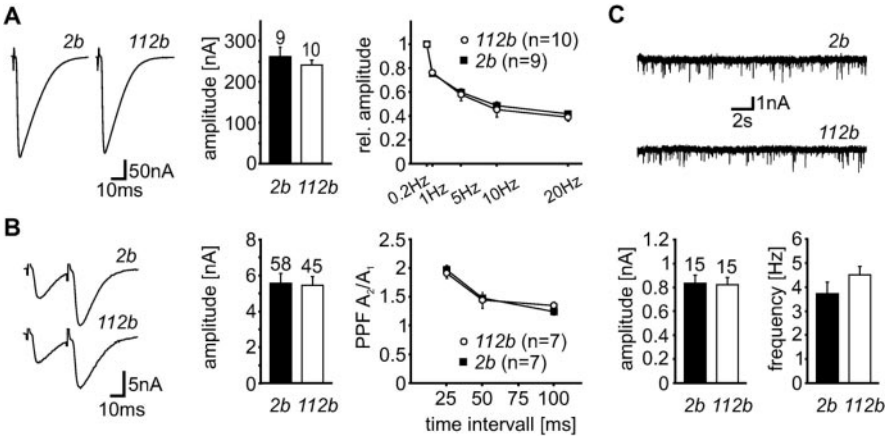

Figure 3. Analysis of basal synaptic properties in *DmGluRA* null mutants. *A*, Evoked synaptic transmission using an extracellular Ca^{2+} concentration of 1.8 mM. Left, Average of 20 consecutive recording traces of EJCs evoked at a frequency of 0.2 Hz in 2b and *DmGluRA*^{112b} larvae. Middle, Mean amplitudes of evoked EJCs (0.2 Hz) were not different in mutant animals compared with control larvae. Right, Mean steady-state amplitude during prolonged trains of stimuli applied at 1, 5, 10, and 20 Hz. No changes were observed in the performance of synaptic transmission at a concentration of 1.8 mM Ca^{2+} in mutant animals. *B*, Evoked synaptic transmission using a reduced extracellular Ca^{2+} concentration of 0.15 mM. Left, Average of 10 consecutive recording traces of EJCs evoked by application of paired stimuli (25 msec interval) at a frequency of 0.1 Hz in 2b and *DmGluRA*^{112b} larvae. Middle, Mean amplitudes of EJCs evoked at a frequency of 0.2 Hz. Similarly reduced mean EJC amplitudes were found for 2b and *DmGluRA*^{112b} larvae. Right, Average PPF using three different interstimulus intervals (25, 50, and 100 msec). PPF was not significantly changed in *DmGluRA*^{112b} animals. *C*, Spontaneous miniature EJCs. Top, Example traces of spontaneously occurring miniature EJCs recorded in *DmGluRA*^{112b} mutants and controls in the presence of 1 μM TTX. Bottom, Mean amplitude (left) as well as mean frequency (right) of spontaneous miniature EJCs appeared undistinguishable from control animals in *DmGluRA*^{112b} mutants. The number of experiments is indicated above the corresponding bar graphs. Data are mean ± SEM.

observed in the control line *DmGluRA*^{2b}. Likewise, immunocytochemical imaging of dissected third instar larvae with the 7G11 antibody also revealed the absence of any detectable NMJ labeling in homozygous *DmGluRA*^{112b} animals (Fig. 1*C*). Thus, we concluded that *DmGluRA*^{112b} represents a protein-null allele, consistent with the characterization of the genomic deletion. Homozygous *DmGluRA*^{112b} mutants are fully viable and develop into fertile adults. This shows that DmGluRA is not an essential gene.

Basal synaptic transmission is normal in *DmGluRA* mutants

Having confirmed that the *DmGluRA*^{112b} mutation represents a null allele, we next assayed whether physiological defects were present in animals lacking mGluR signaling. To answer this question, we used TEVC recordings in body-wall muscles (muscle 6; A3) of wandering third instar larvae. A suction electrode was used to apply brief (~0.4 msec) stimuli to the cut motor nerve, and evoked EJCs were recorded in the muscle. Both low (0.2 Hz) and high (up to 20 Hz) stimulation was used to assay basal synaptic transmission properties.

Using a normal high extracellular Ca^{2+} concentration of 1.8 mM, we observed robust, high-fidelity synaptic transmission in both *DmGluRA*^{2b} control and *DmGluRA*^{112b} mutant animals. The average EJC amplitude was 262.3 ± 22.1 nA ($n = 9$) in *DmGluRA*^{2b} controls and 240.7 ± 13.1 nA ($n = 8$) in *DmGluRA*^{112b} homozygous mutants, which is not significantly different (Fig. 3*A*). Thus, DmGluRA is not detectably required for basal synaptic function. Because metabotropic glutamate receptors are thought to mediate modulation of synaptic transmission during phases of elevated activity (Scanziani et al., 1997; Conn, 2003), we continued the analysis by examining response patterns during stimulation at progressively higher frequencies. The presence of high extracellular Ca^{2+} concentration promotes a strong frequency-dependent depression of EJC amplitudes during application of stimulus trains, whereas low Ca^{2+} concentration allows amplitude facilitation under the same conditions (Zucker and Regehr, 2002). In 1.8 mM Ca^{2+}, EJC amplitudes in *Drosophila* NMJs were similarly depressed in animals of both control and mutant genotypes over a range of different stimulation frequencies (e.g., 40 stimuli at 0.2, 1, and 5 Hz; 60 stimuli at 10 and 20 Hz). EJC amplitudes typically reached a stable level at the end of prolonged stimulus trains. The relative steady-state amplitude ($A_{final}/A_{initial}$, 0.2 Hz) was quantified and compared between control and mutant animals for different stimulation frequencies. Despite our expectations, we did not observe any differences between mutant and control animals with respect to the relative steady-state amplitude (*DmGluRA*^{2b} control, 1 Hz, 75.2 ± 1.4%; 5 Hz, 59.8 ± 1.7%; 10 Hz, 48.6 ± 2.5%; 20 Hz, 41.6 ± 1.6%; $n = 9$; *DmGluRA*^{112b}, 1 Hz, 76.1 ± 1.7%; 5 Hz, 57.8 ± 4.9%; 10 Hz, 45.3 ± 6.3%; 20 Hz, 39.0 ± 3.2%; $n = 8$) (Fig. 3*A*). Thus, the performance of synapses was unchanged in mutant animals in high extracellular Ca^{2+} concentrations (1.8 mM).

The *Drosophila* NMJ is known to strongly compensate for perturbed synaptic transmission in many ways (Davis and Goodman, 1998). Therefore, we reasoned that potential differences in the functional properties of NMJs in *DmGluRA*^{112b} animals might be masked by compensatory changes. To check for changes within the presynaptic transmitter release machinery, we analyzed paired-pulse facilitation (PPF) using a reduced extracellular Ca^{2+} concentration (0.15 mM). Lowering the Ca^{2+} concentration drastically reduced the amplitudes of evoked EJCs. *DmGluRA*^{112b} mutant animals displayed an average evoked EJC amplitude of 5.4 ± 0.5 nA ($n = 45$), comparable with control animals (5.5 ± 0.6 nA; $n = 58$; 0.2 Hz) (Fig. 3*B*). Applying paired stimuli caused an increase in response amplitude to the second stimulus that was similar in mutant and control animals for all of the used interstimulus intervals (ISIs). Specifically, the observed PPF was strongest at an interstimulus interval of 25 msec with values of 1.91 ± 0.09 (A_2/A_1) for *DmGluRA*^{112b} mutants ($n = 7$) and 1.97 ± 0.07 for *DmGluRA*^{2b} controls ($n = 7$) (Fig. 3*B*). For longer ISIs, PPF progressively decreased: at 50 msec ISI, PPF was 1.44 ± 0.15 for *DmGluRA*^{112b} mutants and 1.47 ± 0.03 for *DmGluRA*^{2b} controls; at 100 msec ISI, PPF was 1.35 ± 0.06 for *DmGluRA*^{112b} mutants and 1.24 ± 0.06 for controls. As one of the classical paradigms, PPF has been proven to represent a transient increase in transmitter release, primarily caused by residual calcium (Zucker and Regehr, 2002). Because of the presynaptic nature of PPF, our negative results suggest that these properties of the transmitter release machinery in presynaptic boutons are not dependent on metabotropic glutamate receptor function.

Another instructive parameter describing synaptic function is quantal amplitude, which represents the postsynaptic response to the fusion of a single synaptic vesicle at a single release site (Del Castillo and Katz, 1954). Analysis of miniature EJCs (mEJCs) to estimate the quantal amplitude can highlight differences that are normally masked by compensatory changes in synapse number. We therefore measured mEJC amplitude by recording spontaneous currents in the presence of 1 μM TTX. The mEJC amplitude

was 0.82 ± 0.06 nA for *DmGluRA*^{112b} mutants ($n = 15$) and 0.83 ± 0.06 nA for *DmGluRA*^{2b} controls ($n = 15$) (Fig. 3*C*), with no significant difference. We next analyzed mEJC frequency (1.8 mM Ca^{2+}) and also found no significant difference. The mean frequency of spontaneous mEJCs was 4.5 ± 0.3 Hz for *DmGluRA*^{112b} mutants and 3.7 ± 0.5 Hz for controls ($n = 15$) (Fig. 3*C*). Given that the vesicle fusion probability is unchanged, this result indicates that the number of active release sites is also similar in animals of both genotypes.

In summary, our characterization of the functional properties of glutamatergic NMJs in *DmGluRA*^{112b} mutants did not indicate any changes in basal synaptic transmission. Also, the response patterns of synapses in the presence of 1.8 mM Ca^{2+} were undistinguishable between mutant and control. Therefore, basic synaptic performance is independent of DmGluRA signaling at the *Drosophila* NMJ.

Altered synaptic plasticity during high-frequency stimulation in *DmGluRA* mutants

Because signaling through DmGluRA is not required for basal neurotransmission, we next asked whether it might play a role in synaptic plasticity processes such as facilitation, augmentation, and posttetanic potentiation (PTP). At the *Drosophila* NMJ, these forms of short-term synaptic enhancement are most pronounced in reduced extracellular Ca^{2+} conditions (Zhong and Wu, 1991; Rohrbough et al., 1999), and we therefore used 0.15 mM Ca^{2+} in these studies. We first analyzed synaptic currents evoked by short trains of 20 stimuli applied at different frequencies. To average response amplitudes, stimulus trains were applied five times with resting intervals of 30 sec, with each trial analyzed and averaged.

There was clear synaptic facilitation with a strong frequency dependency in both mutant and control animals: although no significant increase in EJC amplitudes occurred during application of the stimulus trains up to 1 Hz, facilitation was clearly visible at a frequency of 5 Hz and was further increased at 10 Hz (Fig. 4*A*). Most interestingly, facilitation was strongly increased in *DmGluRA*^{112b} mutants compared with control animals. Stimulation at 5 Hz revealed a clear tendency toward stronger facilitation in mutant animals (*DmGluRA*^{2b} control, $A_{20}/A_1 = 1.49 \pm 0.13$, $n = 15$; *DmGluRA*^{112b}, $A_{20}/A_1 = 1.93 \pm 0.16$, $n = 13$), and there was a striking, highly significant, 2.5- to 3-fold facilitation increase during stimulus trains at 10 Hz (*DmGluRA*^{2b} control, $A_{20}/A_1 = 1.83 \pm 0.23$, $n = 16$; *DmGluRA*^{112b}, $A_{20}/A_1 = 5.43 \pm 1.75$, $n = 10$; $p < 0.05$) (Fig. 4*A*, bottom). To control for potential changes in the facilitation properties of mutant animals that might be caused by differences in the genetic background, we repeated the experiment in *DmGluRA* mutant animals of the genotype *DmGluRA*^{112b}*/Df(4)O2*. *Df(4)O2* is a small deficiency of the fourth chromosome covering the *DmGluRA* locus. A similarly dramatically heightened facilitation ($A_{20}/A_1 = 4.75 \pm 1.14$; $n = 11$; $p < 0.05$) could be observed in these animals with an independent genetic background (see Materials and Methods) (Fig. 4*A*, bottom). This is consistent with *DmGluRA*^{112b} being a null allele. Furthermore, we reconfirmed that only the DmGluRA locus is affected in *DmGluRA*^{112b} animals by rescuing the mutant phenotype with presynaptic expression of a DmGluRA transgene. Driving UAS-DmGluRA expression by neuronal BG380-GAL4 resulted in a complete rescue of the observed phenotype. Rescued *DmGluRA*^{112b} larvae showed an average final facilitation of $A_{20}/A_1 = 1.58 \pm 0.21$ ($n = 10$) (Fig. 4*A*, bottom) that was not significantly different from controls. Thus, the presynaptic loss of DmGluRA fully accounts for the dramatically heightened facilitation phenotype.

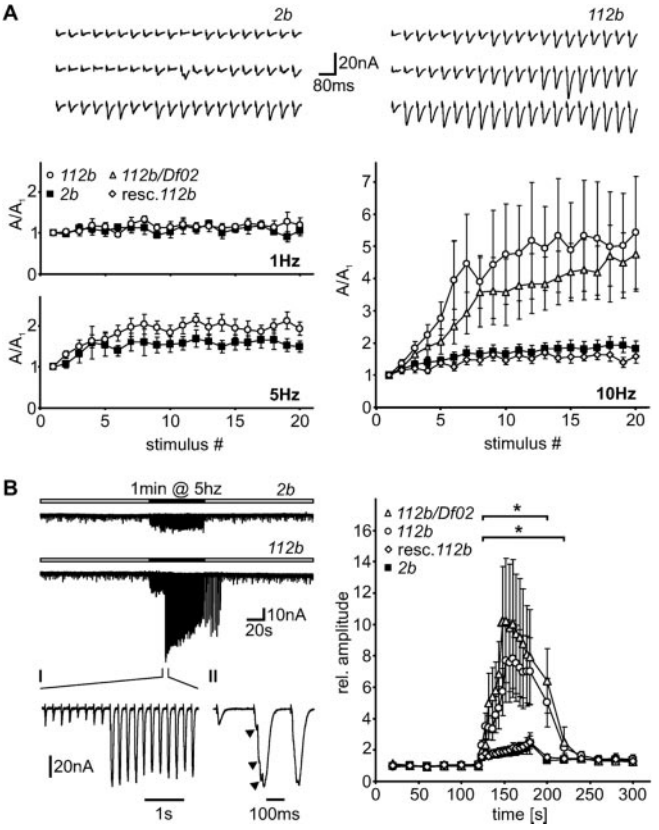

Figure 4. Short-term synaptic enhancement elevated in *DmGluRA* null mutants. *A*, Synaptic facilitation during short trains of 20 pulses applied at different stimulation frequencies (1, 5, 10 Hz; 0.15 mM Ca^{2+}). Top, Example traces showing the development of EJC amplitudes during the application of 20 consecutive stimuli at 10 Hz in *DmGluRA*^{2b} animals (left) and *DmGluRA*^{112b} larvae (right). Bottom, Quantitative analysis. Almost no amplitude facilitation occurred when the stimulus train was applied at 1 Hz (*DmGluRA*^{2b}, $n = 5$; *DmGluRA*^{112b}, $n = 5$). During 5 Hz stimulation, *DmGluRA*^{112b} animals showed slightly stronger facilitation compared with control larvae (*DmGluRA*^{2b}, $n = 15$; *DmGluRA*^{112b}, $n = 13$). Significantly increased facilitation was observed in mutant larvae when stimulation was performed at 10 Hz (*DmGluRA*^{2b}, $n = 16$; *DmGluRA*^{112b}, $n = 10$). Similar results were found for transheterozygous animals of the genotype *DmGluRA*^{112b}*/Df(4)02* ($n = 11$). Rescue animals expressing the transgene DmGluRA under the control of BG380-GAL4 ("*resc. 112b*") were indistinguishable from control ($n = 10$). *B*, Response patterns induced by prolonged tetanic stimulation (5 Hz; 0.15 mM Ca^{2+}) and PTP. Left, Example traces illustrating the typical response behavior of NMJs in *DmGluRA*^{2b} and *DmGluRA*^{112b} larvae during 0.5 Hz test stimulation (white time bars) and tetanic 5 Hz stimulation (black time bar). The response pattern in mutant larvae abruptly changed during 5 Hz stimulation (expanded view I) and exhibited strongly increased and partly asynchronous EJCs (expanded view II; arrows indicate multiple peaks within the increased EJC). Right, Quantitative analysis. On average, amplitudes were significantly (*$p < 0.05$; indicated by brackets) increased in *DmGluRA*^{112b} ($n = 10$; bottom bracket) and *DmGluRA*^{112b}*/Df(4)02* larvae ($n = 10$; top bracket) compared with control ($n = 18$) during 5 Hz stimulation. Rescued mutants with BG380-GAL4 driver ($n = 10$) were indistinguishable from control larvae. Amplitudes persisted at a significantly higher level in mutants for up to 30 sec after tetanic stimulation; longer-lasting PTP was relatively small and unchanged in mutant animals. Data are mean ± SEM.

The *Drosophila* NMJ displays significant augmentation and PTP during prolonged (>30 sec) stimulations at moderate frequencies (5–10 Hz) (Zhong and Wu, 1991; Rohrbough et al., 1999). We therefore assayed whether these persistent forms of synaptic enhancement were also altered in *DmGluRA* mutants. After establishing a stable baseline amplitude during a 2 min basal stimulation period at 0.5 Hz, a 1 min 5 Hz train was applied to induce augmentation, followed by PTP. In control animals, EJC amplitudes during the tetanic stimulation augment significantly

($p < 0.05$) by a factor of 2.42 ± 0.68 ($A_{t = 180\ sec}/A_{pre}$) ($n = 18$). Directly after the stimulus train, control animals display significant potentiation of EJC amplitude ($A_{t = 200\ sec}/A_{pre} = 1.32 \pm 0.11$; $p < 0.05$) that persists at a stable level (at 2 min; $A_{t = 300\ sec}/A_{pre} = 1.35 \pm 0.19$) (Fig. 4*B*). This response profile was dramatically different in mutants compared with control animals. In *DmGluRA* mutants, the response pattern changed completely during the 5 Hz stimulus trains, with the onset of markedly asynchronous EJCs of greatly increased amplitude (Fig. 4*B*). The transition between the elevated short-term facilitation and the dramatically enlarged responses during the augmentation phase was very sharp, without the appearance of EJCs of intermediate amplitude: a "threshold-like" phenomenon. On average, a more than ninefold maximal augmentation during the 5 Hz tetanic stimulation was observed (Fig. 4*B*, right). These enlarged synaptic currents typically showed a multipeak character indicating multiple, nonsummating release events. The threshold-like onset of the increased, asynchronous activity was variable and would appear with unpredictable latencies during the 1 min tetanic stimulus train. After the start of the changed response pattern, we noticed a considerable progressive amplitude depression, very similar to the release behavior observed using higher calcium concentrations. After the 5 Hz stimulation train, EJC amplitudes remained significantly ($p < 0.05$) potentiated for 30 sec or more, before returning to the amplitude level found in control animals (Fig. 4*B*, right). The longer-lasting PTP component in *DmGluRA*^{112b} mutants was comparable with that in control animals ($A_{t = 300\ sec}/A_{pre} = 1.41 \pm 0.29$; $n = 10$). To confirm that the atypical response pattern observed during prolonged stimulation at 5 Hz is specifically caused by the loss of DmGluRA, we repeated the experiment in animals of the genotype *DmGluRA*^{112b}*/Df(4)O2*. The response pattern was indistinguishable from that found in homozygous *DmGluRA*^{112b} mutant animals with an average, maximal augmentation and potentiation of ~10-fold relative to controls ($n = 10$) (Fig. 4*B*, right). We also tested mutant animals that express wild-type UAS-DmGluRA under the control of neuronal BG380-GAL4 for rescue of this phenotype. We never observed large asynchronous responses in these animals, and the final augmentation in rescued *DmGluRA*^{112b} larvae was 2.50 ± 0.39 ($n = 10$) (Fig. 4*B*, right), which is not significantly different from control animals. Thus, the appearance of large facilitated responses is tightly coupled to the absence of DmGluRA in the presynaptic terminal.

In summary, recordings of mutants lacking DmGluRA signaling revealed intriguing changes of synaptic facilitation during application of both short and prolonged stimulus trains. Using a stimulation frequency of 10 Hz, the level of facilitation during short stimulus trains is increased approximately threefold on average in *DmGluRA*^{112b} compared with controls. During prolonged stimulation at 5 Hz, the response pattern dramatically changed in *DmGluRA*^{112b} mutants showing a step-like, ~10-fold increase in EJC amplitude that was accompanied by pronounced asynchrony of the response. After stimulation, synaptic responses remained strongly potentiated in mutants before they suddenly reverted to a normal level of sustained PTP. These data indicate that mGluR signaling is involved in the negative regulation of synaptic transmission during elevated levels of stimulation.

Action potential propagation appears unaffected in *DmGluRA* mutants

Numerous different cellular mechanisms could potentially account for the physiological phenotypes observed in *DmGluRA* mutants. However, the abrupt switch in the response patterns induced by stimulus trains suggests that the loss of mGluR signaling changes the excitability of the presynaptic neuron. The asynchrony of the enlarged EJCs could indicate that multiple action potentials are generated by a single stimulus, leading to the increase in total response amplitude. To investigate possible changes in the generation or propagation of action potentials, we assayed action potentials in the motor nerve by monitoring endogenous action potential trains in mutant and control animals in saline containing 1.8 mM Ca^{2+} (Fig. 5). Extracellular recordings were performed using a suction electrode attached to a differential amplifier.

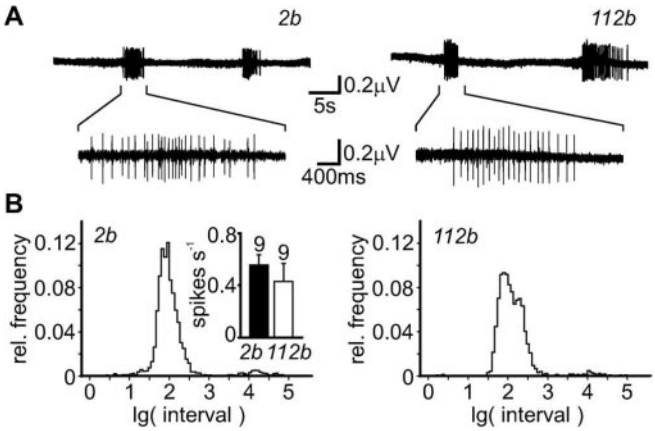

Figure 5. Endogenous action potentials in *DmGluRA* null mutants. *A*, Extracellular recordings in motor nerves of control (*DmGluRA*^{2b}; left) and null mutant (*DmGluRA*^{112b}; right) show endogenous spike trains. Expanded views reveal details of action potential firing. Gross appearance of spike trains is similar in mutant and control animals. *B*, Quantitative analysis of action potential trains. Graphs show distribution of the interval length between consecutive spikes. The maxima of the distributions in control (*DmGluRA*^{2b}; left) and mutant (*DmGluRA*^{112b}; right) lie at ~100 msec (~10 Hz). The distributions median is highly significantly ($p < 0.0001$; Mann–Whitney *U* test) shifted to increased intervals in mutant larvae. The overall spike frequency was not significantly different in mutant and control animals (inset; number of experiments is indicated above bar).

Muscle contractile activity was well correlated with recorded spike trains in both control and mutant larvae. The average spike frequency in *DmGluRA*^{112b} mutants (0.43 ± 0.14 Hz; $n = 9$) was comparable with that found in control larvae (0.56 ± 0.08 Hz; $n = 9$) (Fig. 5*B*, inset). To check for differences in action potential patterns, the intervals between consecutive spikes were analyzed. The distributions of the interspike intervals were skewed, with their medians lying at 58.4 msec for control animals and 72.7 msec for mutant animals, respectively (Fig. 5*B*). This shift to lower action potential spike frequencies in mutant animals was statistically highly significant ($p < 0.0001$; Mann–Whitney *U* test). Consecutive compound action potentials with extremely short interspike intervals, i.e., spike doublets, etc., were extremely rare in both mutant and wild-type larvae, and therefore no clear proof of hyperexcitability was evident. Together, our data suggest that the loss of mGluR signaling has no severe effects on the generation or propagation of action potentials in motor nerves under physiological conditions (1.8 mM Ca^{2+}). The lower frequency of action potentials might indicate additional functions of DmGluRA in the generation of motor activity patterns within the CNS. However, this phenotype would not appear to provide an explanation for the observed defects in NMJ transmission.

Acute pharmacological blockade of DmGluRA has no effect on synaptic properties

DmGluRA signaling could have either an acute or developmental role in the manifestation of changed synaptic properties described previously. If a pharmacological blockade of DmGluRA

signaling could be shown to mimic the phenotypes observed in *DmGluRA* mutants, this would suggest an acute regulation of glutamate release by metabotropic receptors. Most known group II antagonists inhibit DmGluRA with relatively low potency, such as α-methyl-4-phosphonophenylglycine (MPPG) (101.2 μM IC_{50}) (Parmentier et al., 2000). In contrast, LY341495 [2*S*-2amino-2-(1*S*,2*S*-2-carboxycyclopropyl-1-yl)-3-(xanth-9-yl)propanoic acid] is a high-affinity antagonist for the mammalian homologs of DmGluRA, mGluR2, and mGluR3 (Kingston et al., 1998), and we have now shown that this drug also acts as a high-affinity antagonist of DmGluRA in transiently transfected human embryonic kidney HEK293 cells (11.21 ± 1.3 nM IC_{50}; data not shown). We therefore used both MPPG and LY341495 to search for potential effects on synaptic facilitation during short trains of 20 stimuli applied at a frequency of 10 Hz. Before recording, we incubated dissected larvae for 20 min in saline containing the agents.

We first tested the effectiveness of drug delivery under these conditions by incubating preparations in argiotoxin-636, a known open-channel antagonist of the ionotropic glutamate receptors at the *Drosophila* NMJ (Broadie and Bate, 1993). In third instar larvae, incubation with 0.5 μM argiotoxin for 20 min effectively reduced iGluR function to the expected degree (recordings in 1.8 mM Ca^{2+}, mock treatment, 219.5 ± 18.1 nA, $n = 5$; argiotoxin treatment, 67.8 ± 4.4 nA, $n = 5$) (DiAntonio et al., 1999). In contrast, treatment with 200 nM LY341495 did not result in any significant change of basal EJC amplitude during a 0.2 Hz stimulus train (recordings in 0.15 mM Ca^{2+}, control, 10.5 ± 2.8 nA, $n = 5$; LY341495, 8.6 ± 2.0 nA, $n = 7$) and did not significantly increase synaptic facilitation during a 10 Hz stimulus train (control, A_{20}/A_1, 1.38 ± 0.11; LY341495, A_{20}/A_1, 1.67 ± 0.52). Consistently, the antagonist MPPG (1 mM) also did not induce a significant amplitude change (control, 5.6 ± 0.9 nA, $n = 10$; MPPG, 3.4 ± 0.7 nA, $n = 11$) and did not significantly increase facilitation (control, A_{20}/A_1, 1.87 ± 0.21; MPPG, A_{20}/A_1, 2.45 ± 0.30). It is important to note that, with both treatments, there was a definite trend toward increased facilitation, but the change was not significant. Possible interpretations of this result are either (1) that these pharmacological treatments are not effective enough in blocking DmGluR signaling and therefore not comparable with the null *DmGluRA*^{112b} mutant condition, or (2) that mGluR plays a developmental role in the acquisition of presynaptic excitability properties rather than an acute role providing glutamate-feedback regulation. Given the lack of a significant drug effect, the conservative interpretation is for a developmental function of DmGluRA signaling.

DmGluRA signaling modulates synaptic architecture

Long-lasting changes in the efficacy of synaptic transmission are often accompanied by structural changes of synapses (Toni et al., 1999). Hence, apart from their role in modulating transmitter release properties (Anwyl, 1999), mGluRs may also participate in shaping synaptic structure. To our knowledge, only postsynaptic group I mGluRs have been shown to play such a role (Vanderklish and Edelman, 2002). Therefore, we next addressed whether *Drosophila* DmGluRAs were involved in shaping presynaptic terminal morphology. Third instar NMJs were stained with presynaptic markers and assayed for structure using confocal imaging.

The *Drosophila* NMJ exhibited no major structural changes in *DmGluRA*^{112b} null mutants (Fig. 1*C*). Nevertheless, small but significant changes were revealed after closer inspection. *DmGluRA*^{112b} mutant NMJs showed a significant 13.7 ± 3.5% ($n = 26$) reduction in the number of type I synaptic boutons on muscle 6/7 compared with the control line *DmGluRA*^{2b} ($n = 25$; $p < 0.05$) (Fig. 6*A*). Similarly, a larger significant decrease of bouton number was observed on muscles 12 and 13 (23.5 ± 3.3%; $n = 25$; $p < 0.05$; data not shown). Structural changes could not be found in *DmGluRA*^{112b}/+ heterozygous mutants, indicating that the loss-of-function phenotype is recessive. To exclude the possibility that this discrete phenotype was caused by differences in genetic background, we verified that larvae transheterozygous for *DmGluRA*^{112b} and *Df(4)O2* showed a similar decrease in bouton number (at muscle 6/7, 10.02 ± 2.8%; $n = 25$; $p < 0.05$) (Fig. 6*A*). We also verified that muscle surfaces were unaffected in mutants (supplemental material, available at www.jneurosci.org).

Because expression of DmGluRA within the muscle could not be completely excluded, we asked whether the structural defect observed in *DmGluRA*^{112b} mutants was specifically caused by loss of receptor function in the motor neuron. First, we targeted DmGluRA-RNAi with the neuronal GAL4 driver BG380. Despite the fact that DmGluRA staining does not completely disappear under this condition, we observed a small but significant decrease in the number of boutons (6.2 ± 2.5% decrease in bouton number; $n = 74$; $p < 0.05$) (Fig. 6*A*). Second, we verified that presynaptic, but not postsynaptic, expression of a transgene carrying the DmGluRA cDNA restored the wild-type bouton number in mutant animals (relative bouton number, 99.0 ± 7.2%; $n = 9$) (Fig.

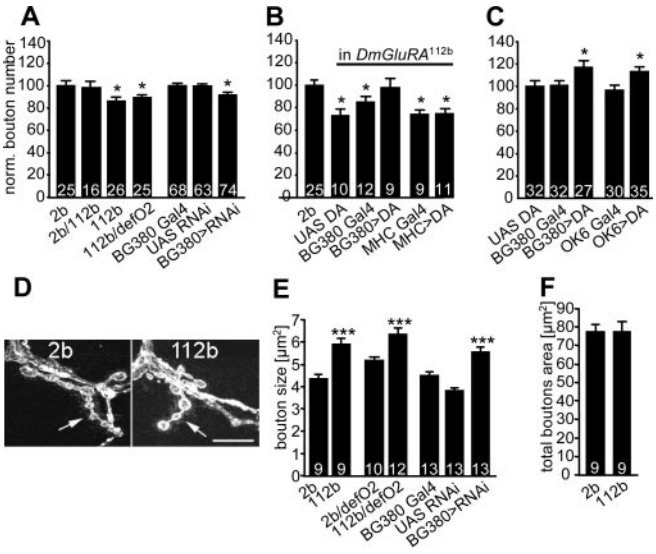

Figure 6. DmGluRA controls the fine structure of NMJ morphology. *A*, Surface normalized (see Materials and Methods) number of synaptic boutons per NMJ (muscle 6/7, segment A2) in different loss of *DmGluRA* function conditions. The number of synaptic boutons is reduced in three distinct genetic combinations: in *DmGluRA*^{112b} homozygous mutants, in larvae with one 112b chromosome facing *Df(4)O2*, and when the DmGluRA-RNAi construct is expressed presynaptically with the BG380-GAL4 driver. Genetic controls (2b and heterozygous BG380-GAL4) are set at 100%. *B*, Presynaptic expression of DmGluRA (DA) in *DmGluRA*^{112b} mutants with the BG380-GAL4 driver restores the wild-type number of boutons, whereas neither postsynaptic expression with MHC-GAL4 nor heterozygous UAS and GAL4 elements alone does. 2b control is set at 100%. *C*, Presynaptic overexpression of DmGluRA with two different GAL4 lines (BG380 and OK6) leads to an increase in bouton number. Heterozygous UAS element alone is set at 100% as control. *D*, Images of Ib terminals (arrows) on muscle 12 in control (2b) and mutant (112b) larvae. Ib boutons are larger in 112b mutants compared with 2b larvae. Scale bar, 10 μm. *E*, Quantification of bouton size in the same loss of function mutants of *DmGluRA* than in *A*. Size of boutons in *DmGluRA* mutants increases. *F*, Total area covered by boutons on muscle 12 corresponding to the sum of individual bouton sizes for each NMJ. Control and mutant NMJs display the same junctional area, indicating a compensation of the defect in bouton number by an increase in bouton size in 112b mutants. For all of the panels, $*p < 0.05$; $**p < 0.01$; $***p < 0.001$. The number of larvae is indicated above the corresponding bar graphs. Data are mean ± SEM.

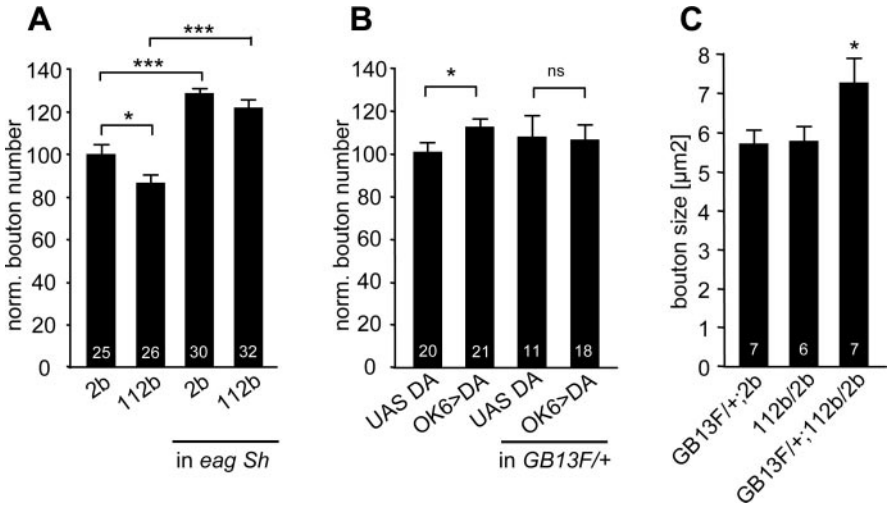

Figure 7. DmGluRA does not interact genetically with *eag Sh* but does interact with *Gβ13F* encoding a subunit of heterotrimeric G-protein. *A*, Number of synaptic boutons per NMJ (muscle 6/7, segment A2) in $DmGluRA^{112b}$ mutants and double mutants $eag^1\ Sh^{120}$; $DmGluRA^{112b}$ compared with their control. 2b control is set at 100%. The increase in bouton number characterizing $eag^1\ Sh^{120}$ phenotype is seen both in wild-type (2b) or *DmGluRA* mutant (112b) background. *B*, Number of synaptic boutons per NMJ (muscle 6/7, segment A2) when DmGluRA (DA) is overexpressed presynaptically in wild-type or heterozygote condition for $Gβ13F^{Δ[supi]1–96A}$ mutation. When one copy of *Gβ13F* subunit is missing, overexpression of DmGluRA does not lead yet to any significant increase in bouton number. *C*, Mean bouton area in double heterozygotes for $DmGluRA^{112b}$ and $Gβ13F^{Δ[supi]1–96A}$ mutations. Each heterozygous mutation alone does not modify bouton area, whereas double heterozygotes display a bouton area increase, similarly to *DmGluRA* mutants. The number of larvae is indicated above the corresponding bar graphs. Data are mean ± SEM.

6*B*). Together, these results indicate that the mutant phenotype is exclusively caused by a loss of DmGluRA signaling in motor neurons. We further investigated whether a direct correlation between availability of DmGluRA and the morphology of the presynaptic terminal exists at the *Drosophila* NMJ. Most interestingly, we found that synaptic bouton number increased significantly when DmGluRA was overexpressed specifically in neurons by two independent GAL4 drivers: OK6, 12.6 ± 4.1% ($n = 21$; $p < 0.05$) and BG380, 15.8 ± 5.7% ($n = 27$; $p < 0.05$) (Fig. 6*C*). These observations show that an increased amount of presynaptic DmGluRA causes an upregulation of synaptic bouton number.

Previous work has indicated a negative correlation between NMJ bouton number and bouton size in different genetic conditions (Roos et al., 2000). We therefore tested for such a negative correlation in *DmGluRA* mutants. We quantified the maximal area of the z-projection of all of the type Ib boutons for each NMJ studied. Because of its advantageous structural properties for imaging of boutons, we focused our analysis on muscle 12, although synaptic boutons on muscle 6/7 showed qualitatively the same results (data not shown). $DmGluRA^{112b}$ mutants exhibited clearly larger boutons (mean area, 5.89 ± 0.30 μm^2; $n = 9$) compared with $DmGluRA^{2b}$ control animals (mean area, 4.33 ± 0.18 μm^2; $n = 9$; $p < 0.001$) (Fig. 6*D*,*E*). The same result was obtained for $DmGluRA^{112b}/Df(4)O2$ mutants compared with $DmGluRA^{2b}/Df(4)O2$ controls (6.32 ± 0.30 μm^2, $n = 11$; 5.16 ± 0.20 μm^2, $n = 10$; $p < 0.001$) and also when a DmGluRA-RNAi construct was driven presynaptically (5.54 ± 0.25 μm^2; $n = 13$; $p < 0.001$) (Fig. 6*E*).

In summary, these data show that a loss of presynaptic DmGluRA function leads to a reduction in bouton number but an increase in bouton size. Because it might be reasoned that the increase in bouton size to some degree compensates for the decrease in bouton number, we calculated the total bouton area for animals of each genotype. The total bouton area was not significantly different between $DmGluRA^{2b}$ controls (78.01 ± 4.1 μm^2; $n = 9$) and $DmGluRA^{112b}$ mutants (76.56 ± 5.35 μm^2; $n = 9$; $p = 0.83$) (Fig. 6*F*), indicating that bouton formation, but not total NMJ synaptic size, is affected in *DmGluRA* mutants.

DmGluRA function is independent of $eag^1\ Sh^{120}$ but requires the G-protein subunit *Gβ13F*

An increase in bouton number is a characteristic feature of some hyperactive mutants, such as the potassium channel double-mutant $eag^1\ Sh^{120}$ (Budnik et al., 1990; Zhong et al., 1992). Because DmGluRA may be a sensor of activity-dependent glutamate release, we therefore assayed whether the structural overgrowth caused by *eag Sh* hyperactivity might be dependent on mGluR signaling. To that purpose, we crossed $DmGluRA^{112b}$ into the $eag^1\ sh^{120}$ mutant background. In triple mutants of eag^1Sh^{120}; $DmGluRA^{112b}$, the NMJ overgrowth characteristic of $eag^1\ sh^{120}$ alone persisted (Fig. 7*A*). The bouton number in $eag^1\ Sh^{120}$; $DmGluRA^{112b}$ mutants was 120.0 ± 3.1 ($n = 34$), whereas the $DmGluRA^{112b}$ homozygous mutants alone had an average bouton number of 86.3 ± 3.5 ($n = 25$) (Fig. 7*A*). This result suggests that DmGluRA does not participate in the processes underlying the structural changes caused by hyperactivity in these potassium channel mutants.

Group II metabotropic receptors are known to couple to G_i/G_o G-proteins, which dissociate into α-subunit and βγ-subunit complex on activation, and thereby release two different effectors (Cabrera-Vera et al., 2003). We took advantage of an existing mutation in the Gβ13F subunit, which is known to interact with $Gα_i$ subunit (Schaefer et al., 2001), to investigate the implication of the βγ-subunit complex in DmGluRA signaling. To that purpose, we tested whether the increase in bouton number obtained with presynaptic overexpression of DmGluRA with OK6-GAL4 would persist with only one functional copy of the *Gβ13F* gene. Although there was no significant change in NMJ bouton number caused by deleting one copy of *Gβ13F* (Fig. 7*B*), we found that deletion of one copy of *Gβ13F* suppressed the increase in bouton number induced by DmGluRA overexpression (Fig. 7*B*). This genetic interaction suggests that *Gβ13F* is required for DmGluRA-mediated modulation of synaptic structure.

We further verified the genetic interaction between *DmGluRA* and *Gβ13F* by studying the structural phenotype of the transheterozygote $DmGluRA^{112b}/+$; $Gβ13F^{Δ1–96A}/+$. Each mutation in a heterozygous condition had no effect on either bouton number or bouton size (Figs. 6*A*, 7*B*,*C*). However, animals heterozygous for both mutations phenocopied the effect on bouton size caused by a complete lack of DmGluRA signaling (Fig. 7*C*), whereas the bouton number remained unchanged (100.5 ± 3.2, $n = 29$ for *Gβ13F*/+;2b/+; 97.2 ± 4.0, $n = 27$ for *Gβ13F*/+; 112b/+; NS). Thus, there is a positive genetic interaction between *DmGluRA* and *Gβ13F* loss-of-function mutations, indicating that *DmGluRA* and *Gβ13F* act in the same signaling pathway for structural modulation of the NMJ. Together, these data indicate

that a $G\beta\gamma$ complex, which comprises the *Gβ13F* subunit, acts downstream of DmGluRA in the control of synaptic architecture.

Discussion

DmGluRA inhabits presynaptic periactive zones, like vertebrate group II mGluRs

DmGluRA is the only functional metabotropic glutamate receptor encoded by the sequenced *Drosophila* genome. Thus, mutation of this single gene allows us to assay the entire requirement of metabotropic glutamate signaling throughout the animal. In this study, we generated the first *DmGluRA* mutations. Null mutants are viable, fertile, and appear to behave normally. We focused on mGluR roles at the well characterized glutamatergic NMJ. DmGluRA is expressed at the NMJ, although at relatively low abundance. Transgenic RNAi constructs expressed in either the presynaptic or postsynaptic cell revealed that DmGluRA is primarily presynaptic, consistent with localization of its vertebrate orthologs, group II mGluRs (mGlu2/3) (Neki et al., 1996). A presynaptic localization is also consistent with Zhang et al. (1999), who reported a group II agonist-induced presynaptic enhancement of synaptic transmission at the *Drosophila* NMJ of first instar larvae.

DmGluRA receptors were not distributed homogeneously in synaptic boutons but rather appear in discrete patches that do not overlap with ionotropic glutamate receptors inhabiting the postsynaptic specialization apposing presynaptic glutamate release sites. Thus, DmGluRA receptors appear to be mostly excluded from release sites and rather inhabit the periactive zone. These results fit well with the reported ultrastructural localization of vertebrate group II mGluRs, which are known to be excluded from glutamate release zones (Lujan et al., 1997; Tamaru et al., 2001). This distribution suggests that DmGluRA receptors are positioned to function as presynaptic autoreceptors, to sense glutamate spilling out of the active signaling zone.

DmGluRA modulates frequency-dependent glutamatergic transmission

DmGluRA receptors are well positioned to modulate presynaptic release properties. Numerous reports have shown that the application of group II mGluR agonists inhibits synaptic transmission at various glutamatergic synapses (for review, see Conn and Pin, 1997; Anwyl, 1999), suggesting that mGluR mutants display enhanced synaptic transmission. However, mGluR2 knock-out mice show no modifications of basal synaptic transmission or paired-pulse facilitation at mossy fiber–CA3 synapses (Yokoi et al., 1996). Similarly, electrophysiological characterization of *DmGluRA* mutants revealed no changes in basal synaptic transmission or paired-pulse facilitation at the *Drosophila* NMJ. Thus, mGluR signaling is not involved in maintenance–regulation of basal neurotransmission. Nevertheless, mGluRs may mediate modulation processes at elevated activity levels. Indeed, activation of postsynaptic group I mGluRs critically depends on duration and frequency of synaptic activity (Batchelor and Garthwaite, 1997). Likewise, Scanziani et al. (1997) proposed activity-dependent activation of presynaptic mGluR2 on mossy fibers caused by glutamate spillover from adjacent synapses, suggesting that presynaptic mGluRs are activated only during elevated activity. Nevertheless, synaptic transmission in *DmGluRA* mutants was unchanged at higher stimulation frequencies (1–20 Hz) in physiological conditions. We cannot exclude the possibility that differences in the performance of mutant synapses may arise under specific stimulation conditions. For example, in the lateral perforant path of the dentate gyrus, application of a group III agonist influences synaptic depression only during prolonged stimulation at frequencies higher than 5 Hz (Rush et al., 2002). Thus, presynaptic mGluRs may regulate neurotransmission only during certain, tightly defined conditions.

A general feature of many synapses, including the *Drosophila* NMJ, is that low extracellular Ca^{2+} concentration (e.g., 0.15 mM) alleviates synaptic depression and permits the manifestation of synaptic facilitation. Under this condition, we observed a strong requirement for mGluR signaling: in *DmGluRA* mutants, a striking, approximately threefold increase in facilitation during short trains of 10 Hz stimulation was observed. In general, facilitation is thought to be caused by presynaptic accumulation of Ca^{2+}, which strengthens synaptic transmission by promoting Ca^{2+}-sensitive steps of exocytosis. However, altering Ca^{2+} entry or Ca^{2+} sensitivity should affect basal transmission and paired-pulse facilitation, but both parameters were unchanged in *DmGluRA* mutants. Thus, other defective mechanisms must account for the facilitation defect. The most probable explanation is altered presynaptic excitability properties. Hyperexcitable *Drosophila* mutants, including *Hyperkinetic*, *bemused*, *frequenin*, and *para*-overexpressing flies have all been demonstrated to exhibit increased onset rates during facilitation (Stern and Ganetzky, 1989; Stern et al., 1990, 1995; Rivosecchi et al., 1994), indicating that facilitation is significantly altered by excitability changes. The hypothesis that DmGluRA signaling regulates presynaptic excitability seems particularly intriguing when considering the described changes in response patterns observed in mutants during more prolonged (1 min, 5 Hz) stimulation: *DmGluRA* mutants show a striking threshold-like change in response pattern, resulting in extraordinarily increased EJC amplitudes that have an asynchronous event probability. The sharp transition between the initially relatively mild enhancement of facilitation and the abruptly 10-fold increased responses is most readily explained by a change in excitability properties, allowing the generation of multiple spikes after a single stimuli. Most interestingly, identically changed response patterns have been reported in *frequenin*-overexpressing larvae (Rivosecchi et al., 1994), which have been termed "large facilitated responses." Frequenin overexpression modulates the properties of presynaptic potassium channels (Pongs et al., 1993; Nakamura et al., 2001), making these channels a likely target for DmGluRA regulation. Similarly, in vertebrates, activation of mGluRs can induce the modulation of presynaptic voltage-gated ion channels (Anwyl, 1999).

We investigated putative excitability changes in *DmGluRA* mutants by extracellularly recording endogenous action potential trains in the motor nerve using physiological conditions (1.8 mM Ca^{2+}). Spike trains in mutants were similar to controls and did not contain multiple, closely successive spike events that would be indicative of hyperexcitability. Therefore, generally elevated excitability is unlikely. DmGluRA-dependent changes in excitability might be restricted to synaptic boutons in which DmGluRA is localized. In addition, elevated nerve excitability may occur in *DmGluRA* mutants only with reduced Ca^{2+}, when the excitability of motor nerves is already increased by changing the surface charge as a result of the removal of divalent cations. Unfortunately, technical limitations have so far prevented us from assaying action potentials under the same conditions found to promote the synaptic phenotype. Interestingly, we found that *DmGluRA* mutants fired action potentials within trains with a significantly reduced frequency. This change may reflect altered excitability within the motor neuron or changed activity patterns within the CNS. DmGluRA is expressed in the ventral nerve cord neuropil (data not shown), in which it could potentially modulate neuronal activity.

The dramatic changes in neurotransmitter release during high-frequency stimulation are most readily explained by abolishment of a critical presynaptic negative feedback mechanism in mutant animals. However, we were unable to mimic phenotypes by acute application of mGluR antagonists (MPPG or LY341495). A particular important caveat is that pharmacological inhibition may simply not be effective enough to fully recapitulate phenotypes observed in null mutants; therefore, we do not exclude the possibility of an acute feedback mechanism. From this perspective, we note that results presented here from third instar contradict a study by Zhang et al. (1999) in the early first instar describing acute increase in miniature frequency induced by group II agonists and partial blockade of evoked EJCs by antagonists. This difference may be attributable to the absence of the convoluted subsynaptic reticulum in the first instar, which may be causing a significant experimental limitation to drug application in the third instar. Indeed, we observed that the iGluR blocker argiotoxin-636 results in a 70% block in receptor function in the third instar, in accordance with DiAntonio et al. (1999), whereas the same toxin eliminates iGluR function in the more accessible first instar (Broadie and Bate, 1993). These caveats aside, a developmental role for mGluR signaling is certainly possible. For example, thalamic mGluR1 shows a developmental reorganization, in which its subcellular distribution changes (Liu et al., 1998). Intriguingly, this reorganization is correlated to a change in the properties of glutamatergic synapses at maturing thalamic neurons (Golshani et al., 1998).

DmGluRA modulates fine synaptic architecture

Drosophila NMJ structure is sculpted by developmental cues and neuronal activity. Increased neuronal activity positively correlates with an increased number of synaptic boutons, as illustrated by *eag Sh* or *Hk eag* hyperexcitable mutants. However, other hyperexcitable mutants, such as *frequenin*-overexpressing larvae, display an opposite phenotype, i.e., a reduction in bouton number and an increase in bouton size (Angaut-Petit et al., 1998). Thus, different mechanisms must be involved in linking activity to synaptic morphology.

Here, we show that *DmGluRA* null mutants display altered presynaptic excitability and an ~10–20% decreased number of synaptic boutons. It is debatable whether and how structural and physiological phenotypes in *DmGluRA* mutants are mechanistically linked. It is uncertain whether the morphological changes significantly influence the functional properties or whether the suspected excitability change is responsible for the subtle structural changes. Experiments using DmGluRA overexpression and DmGluRA-RNAi indicate a significant correlation between presynaptic DmGluRA level and bouton differentiation. Moreover, *DmGluRA* mutants exhibit an increased bouton size, compensating for the decreased bouton number. Thus, DmGluRA modulates bouton number but has no detectable impact on the overall bouton area of the NMJ. Consistently, the frequency of spontaneous mEJCs was unchanged in *DmGluRA* mutants, suggesting that functional release site density is normal. Such a role of a presynaptic group II mGluR in the fine control of synaptic architecture was still unknown. It could be of growing interest, because human group II/III mGluRs have been shown to be drug targets in numerous psychiatric and neurological disorders, such as schizophrenia and seizure disorders (Marek, 2004). Interestingly, such disorders are characterized by the presence of subtle synaptic abnormalities (Blanpied and Ehlers, 2004).

DmGluRA mutants share both electrophysiological and morphological phenotypes with *frequenin*-overexpressing larvae. We have shown that the *eag Sh* structural phenotype does not depend on the presence of DmGluRA. This suggests that similar signaling pathways are affected in *DmGluRA* and *frequenin* mutants and that these pathways differ from those affected in *eag Sh* mutants. We started to dissect the transduction pathway activated by DmGluRA: here, we show that the Gβ13F subunit is required to mediate the morphological changes.

References

Aberle H, Haghighi AP, Fetter RD, McCabe BD, Magalhaes TR, Goodman CS (2002) Wishful thinking encodes a BMP type II receptor that regulates synaptic growth in *Drosophila*. Neuron 33:545–558.

Angaut-Petit D, Toth P, Rogero O, Faille L, Tejedor FJ, Ferrus A (1998) Enhanced neurotransmitter release is associated with reduction of neuronal branching in a *Drosophila* mutant overexpressing frequenin. Eur J Neurosci 10:423–434.

Anwyl R (1999) Metabotropic glutamate receptors: electrophysiological properties and role in plasticity. Brain Res Brain Res Rev 29:83–120.

Batchelor AM, Garthwaite J (1997) Frequency detection and temporally dispersed synaptic signal association through a metabotropic glutamate receptor pathway. Nature 385:74–77.

Baude A, Nusser Z, Roberts JD, Mulvihill E, McIlhinney RA, Somogyi P (1993) The metabotropic glutamate receptor (mGluR1 alpha) is concentrated at perisynaptic membrane of neuronal subpopulations as detected by immunogold reaction. Neuron 11:771–787.

Blanpied TA, Ehlers MD (2004) Microanatomy of dendritic spines: emerging principles of synaptic pathology in psychiatric and neurological disease. Biol Psychiatry 55:1121–1127.

Broadie KS, Bate M (1993) Development of the embryonic neuromuscular synapse of *Drosophila melanogaster*. J Neurosci 13:144–166.

Budnik V, Zhong Y, Wu CF (1990) Morphological plasticity of motor axons in *Drosophila* mutants with altered excitability. J Neurosci 10:3754–3768.

Budnik V, Koh YH, Guan B, Hartmann B, Hough C, Woods D, Gorczyca M (1996) Regulation of synapse structure and function by the *Drosophila* tumor suppressor gene dlg. Neuron 17:627–640.

Cabrera-Vera TM, Vanhauwe J, Thomas TO, Medkova M, Preininger A, Mazzoni MR, Hamm HE (2003) Insights into G protein structure, function, and regulation. Endocr Rev 24:765–781.

Conn PJ (2003) Physiological roles and therapeutic potential of metabotropic glutamate receptors. Ann NY Acad Sci 1003:12–21.

Conn PJ, Pin JP (1997) Pharmacology and functions of metabotropic glutamate receptors. Annu Rev Pharmacol Toxicol 37:205–237.

Cryderman DE, Cuaycong MH, Elgin SC, Wallrath LL (1998) Characterization of sequences associated with position-effect variegation at pericentric sites in *Drosophila* heterochromatin. Chromosoma 107:277–285.

Davis GW, Goodman CS (1998) Genetic analysis of synaptic development and plasticity: homeostatic regulation of synaptic efficacy. Curr Opin Neurobiol 8:149–156.

Del Castillo J, Katz B (1954) Action, and spontaneous release, of acetylcholine at an inexcitable nerve-muscle junction. J Physiol (Lond) 126:27P.

DiAntonio A, Petersen SA, Heckmann M, Goodman CS (1999) Glutamate receptor expression regulates quantal size and quantal content at the *Drosophila* neuromuscular junction. J Neurosci 19:3023–3032.

Golshani P, Warren RA, Jones EG (1998) Progression of change in NMDA, non-NMDA, and metabotropic glutamate receptor function at the developing corticothalamic synapse. J Neurophysiol 80:143–154.

Gonzalez-Gaitan M, Jackle H (1997) Role of *Drosophila* alpha-adaptin in presynaptic vesicle recycling. Cell 88:767–776.

Hou D, Suzuki K, Wolfgang WJ, Clay C, Forte M, Kidokoro Y (2003) Presynaptic impairment of synaptic transmission in *Drosophila* embryos lacking Gsα. J Neurosci 23:5897–5905.

Kingston AE, Ornstein PL, Wright RA, Johnson BG, Mayne NG, Burnett JP, Belagaje R, Wu S, Schoepp DD (1998) LY341495 is a nanomolar potent and selective antagonist of group II metabotropic glutamate receptors. Neuropharmacology 37:1–12.

Koenig JH, Ikeda K (1996) Synaptic vesicles have two distinct recycling pathways. J Cell Biol 135:797–808.

Lee T, Lee A, Luo L (1999) Development of the *Drosophila* mushroom bodies: sequential generation of three distinct types of neurons from a neuroblast. Development 126:4065–4076.

Liu XB, Munoz A, Jones EG (1998) Changes in subcellular localization of

metabotropic glutamate receptor subtypes during postnatal development of mouse thalamus. J Comp Neurol 395:450–465.

Lujan R, Roberts JD, Shigemoto R, Ohishi H, Somogyi P (1997) Differential plasma membrane distribution of metabotropic glutamate receptors mGluR1 alpha, mGluR2 and mGluR5, relative to neurotransmitter release sites. J Chem Neuroanat 13:219–241.

Lynch MA (2004) Long-term potentiation and memory. Physiol Rev 84:87–136.

Marek GJ (2004) Metabotropic glutamate 2/3 receptors as drug targets. Curr Opin Pharmacol 4:18–22.

Marrus SB, Portman SL, Allen MJ, Moffat KG, DiAntonio A (2004) Differential localization of glutamate receptor subunits at the *Drosophila* neuromuscular junction. J Neurosci 24:1406–1415.

Mitri C, Parmentier ML, Pin JP, Bockaert J, Grau Y (2004) Divergent evolution in metabotropic glutamate receptors. A new receptor activated by an endogenous ligand different from glutamate in insects. J Biol Chem 279:9313–9320.

Nakamura TY, Pountney DJ, Ozaita A, Nandi S, Ueda S, Rudy B, Coetzee WA (2001) A role for frequenin, a Ca^{2+}-binding protein, as a regulator of Kv4 K^+-currents. Proc Natl Acad Sci USA 98:12808–12813.

Neki A, Ohishi H, Kaneko T, Shigemoto R, Nakanishi S, Mizuno N (1996) Pre- and postsynaptic localization of a metabotropic glutamate receptor, mGluR2, in the rat brain: an immunohistochemical study with a monoclonal antibody. Neurosci Lett 202:197–200.

Ozawa S, Kamiya H, Tsuzuki K (1998) Glutamate receptors in the mammalian central nervous system. Prog Neurobiol 54:581–618.

Packard M, Mathew D, Budnik V (2003) Wnts and TGF beta in synaptogenesis: old friends signalling at new places. Nat Rev Neurosci 4:113–120.

Panneels V, Eroglu C, Cronet P, Sinning I (2003) Pharmacological characterization and immunoaffinity purification of metabotropic glutamate receptor from *Drosophila* overexpressed in Sf9 cells. Protein Expr Purif 30:275–282.

Parmentier ML, Pin JP, Bockaert J, Grau Y (1996) Cloning and functional expression of a *Drosophila* metabotropic glutamate receptor expressed in the embryonic CNS. J Neurosci 16:6687–6694.

Parmentier ML, Galvez T, Acher F, Peyre B, Pellicciari R, Grau Y, Bockaert J, Pin JP (2000) Conservation of the ligand recognition site of metabotropic glutamate receptors during evolution. Neuropharmacology 39:1119–1131.

Petersen SA, Fetter RD, Noordermeer JN, Goodman CS, DiAntonio A (1997) Genetic analysis of glutamate receptors in *Drosophila* reveals a retrograde signal regulating presynaptic transmitter release. Neuron 19:1237–1248.

Pongs O, Lindemeier J, Zhu XR, Theil T, Engelkamp D, Krah-Jentgens I, Lambrecht HG, Koch KW, Schwemer J, Rivosecchi R, Mallart A, Galceran J, Canal I, Barbas JA, Ferrus A (1993) Frequenin—a novel calcium-binding protein that modulates synaptic efficacy in the *Drosophila* nervous system. Neuron 11:15–28.

Ramaekers A, Parmentier ML, Lasnier C, Bockaert J, Grau Y (2001) Distribution of metabotropic glutamate receptor DmGlu-A in *Drosophila melanogaster* central nervous system. J Comp Neurol 438:213–225.

Rheuben MB, Yoshihara M, Kidokoro Y (1999) Ultrastructural correlates of neuromuscular junction development. In: Neuromuscular junctions in *Drosophila* (Budnik V, Gramates LS, eds), pp 69–92. San Diego: Academic.

Rivosecchi R, Pongs O, Theil T, Mallart A (1994) Implication of frequenin in the facilitation of transmitter release in *Drosophila*. J Physiol (Lond) 474:223–232.

Robertson HM, Preston CR, Phillis RW, Johnson-Schlitz DM, Benz WK, Engels WR (1988) A stable genomic source of P element transposase in *Drosophila melanogaster*. Genetics 118:461–470.

Rohrbough J, Pinto S, Mihalek RM, Tully T, Broadie K (1999) latheo, a *Drosophila* gene involved in learning, regulates functional synaptic plasticity. Neuron 23:55–70.

Rohrbough J, O'Dowd DK, Baines RA, Broadie K (2003) Cellular bases of behavioral plasticity: establishing and modifying synaptic circuits in the *Drosophila* genetic system. J Neurobiol 54:254–271.

Roos J, Hummel T, Ng N, Klambt C, Davis GW (2000) *Drosophila* Futsch regulates synaptic microtubule organization and is necessary for synaptic growth. Neuron 26:371–382.

Rush AM, Kilbride J, Rowan MJ, Anwyl R (2002) Presynaptic group III mGluR modulation of short-term plasticity in the lateral perforant path of the dentate gyrus in vitro. Brain Res 952:38–43.

Saitoe M, Schwarz TL, Umbach JA, Gundersen CB, Kidokoro Y (2001) Absence of junctional glutamate receptor clusters in *Drosophila* mutants lacking spontaneous transmitter release. Science 293:514–517.

Scanziani M, Salin PA, Vogt KE, Malenka RC, Nicoll RA (1997) Use-dependent increases in glutamate concentration activate presynaptic metabotropic glutamate receptors. Nature 385:630–634.

Schaefer M, Petronczki M, Dorner D, Forte M, Knoblich JA (2001) Heterotrimeric G proteins direct two modes of asymmetric cell division in the *Drosophila* nervous system. Cell 107:183–194.

Schuster CM, Ultsch A, Schloss P, Cox JA, Schmitt B, Betz H (1991) Molecular cloning of an invertebrate glutamate receptor subunit expressed in *Drosophila* muscle. Science 254:112–114.

Schuster CM, Davis GW, Fetter RD, Goodman CS (1996a) Genetic dissection of structural and functional components of synaptic plasticity. I. Fasciclin II controls synaptic stabilization and growth. Neuron 17:641–654.

Schuster CM, Davis GW, Fetter RD, Goodman CS (1996b) Genetic dissection of structural and functional components of synaptic plasticity. II. Fasciclin II controls presynaptic structural plasticity. Neuron 17:655–667.

Shigemoto R, Kinoshita A, Wada E, Nomura S, Ohishi H, Takada M, Flor PJ, Neki A, Abe T, Nakanishi S, Mizuno N (1997) Differential presynaptic localization of metabotropic glutamate receptor subtypes in the rat hippocampus. J Neurosci 17:7503–7522.

Sigrist SJ, Thiel PR, Reiff DF, Schuster CM (2002) The postsynaptic glutamate receptor subunit DGluR-IIA mediates long-term plasticity in *Drosophila*. J Neurosci 22:7362–7372.

Sone M, Suzuki E, Hoshino M, Hou D, Kuromi H, Fukata M, Kuroda S, Kaibuchi K, Nabeshima Y, Hama C (2000) Synaptic development is controlled in the periactive zones of *Drosophila* synapses. Development 127:4157–4168.

Stern M, Ganetzky B (1989) Altered synaptic transmission in *Drosophila* hyperkinetic mutants. J Neurogenet 5:215–228.

Stern M, Kreber R, Ganetzky B (1990) Dosage effects of a *Drosophila* sodium channel gene on behavior and axonal excitability. Genetics 124:133–143.

Stern M, Blake N, Zondlo N, Walters K (1995) Increased neuronal excitability conferred by a mutation in the *Drosophila* bemused gene. J Neurogenet 10:103–118.

Tamaru Y, Nomura S, Mizuno N, Shigemoto R (2001) Distribution of metabotropic glutamate receptor mGluR3 in the mouse CNS: differential location relative to pre- and postsynaptic sites. Neuroscience 106:481–503.

Toni N, Buchs PA, Nikonenko I, Bron CR, Muller D (1999) LTP promotes formation of multiple spine synapses between a single axon terminal and a dendrite. Nature 402:421–425.

Vanderklish PW, Edelman GM (2002) Dendritic spines elongate after stimulation of group 1 metabotropic glutamate receptors in cultured hippocampal neurons. Proc Natl Acad Sci USA 99:1639–1644.

Yokoi M, Kobayashi K, Manabe T, Takahashi T, Sakaguchi I, Katsuura G, Shigemoto R, Ohishi H, Nomura S, Nakamura K, Nakao K, Katsuki M, Nakanishi S (1996) Impairment of hippocampal mossy fiber LTD in mice lacking mGluR2. Science 273:645–647.

Yuste R, Bonhoeffer T (2001) Morphological changes in dendritic spines associated with long-term synaptic plasticity. Annu Rev Neurosci 24:1071–1089.

Zhang D, Kuromi H, Kidokoro Y (1999) Activation of metabotropic glutamate receptors enhances synaptic transmission at the *Drosophila* neuromuscular junction. Neuropharmacology 38:645–657.

Zhong Y, Wu CF (1991) Altered synaptic plasticity in *Drosophila* memory mutants with a defective cyclic AMP cascade. Science 251:198–201.

Zhong Y, Budnik V, Wu CF (1992) Synaptic plasticity in *Drosophila* memory and hyperexcitable mutants: role of cAMP cascade. J Neurosci 12:644–651.

Zucker RS, Regehr WG (2002) Short-term synaptic plasticity. Annu Rev Physiol 64:355–405.